Space Shuttle Performance with a Heads-Up Ascent

S. W. Millard*
NASA Johnson Space Center, Houston, Texas

A method of increasing the space transportation system (STS) lift capability by flying the Space Shuttle vehicle in a heads-up, conventional airplane-piloting attitude during the first-stage atmospheric flight as opposed to the current heads-down attitude is presented. It is revealed that the STS lift capability and solid rocket motor burnrate definition are sensitive to the magnitude and direction of normal aerodynamic force acting on the Space Shuttle vehicle during atmospheric ascent. The STS operational trajectory design angle of attack will permit increases in the solid rocket motor (SRM) burnrate definition and STS lift capability for the proposed heads-up ascent when compared to the current heads-down ascent. For a heads-up ascent, the SRM burnrate can be increased 7% with a corresponding 4000 lb increase in STS lift capability. A comparison of the heads-up and heads-down ascent reveals similar performance trades for changes in trajectory-shaping parameters, SRM and Space Shuttle main engine (SSME) performance characteristics.

Nomenclature

α_w = wind relative angle of attack
β_w = wind relative angle of sideslip
μ = bank angle
α_N = nominal angle of attack
α_T = tailwind angle of attack
α_H = headwind angle of attack
V_∞ = freestream velocity
$\bar{q}$ = dynamic pressure
R = resultant force vector
α_s = thrust vector angle of attack
F_A = aero axial force
F_N = aero normal force
F_{SSME} = Space Shuttle main engine force
F_{SRB} = solid rocket booster force
γ = Earth-relative flight path angle
mg = gravitational weight
I = inertial axis
W = wind axis
B = SSV body axis
WIT = wind-to-inertial axis transformation matrix
BWT = body-to-wind axis transformation matrix
BIT = body-to-inertial axis transformation matrix
A_{zw} = wind-relative flight azimuth
θ = inertial body-pitch attitude
ψ = inertial body-yaw attitude
ϕ = inertial body-roll attitude

Acronyms

ET = external tank
ETR = Eastern test range
FWC = filament wound case
ips = in./s
MECO = main engine cutoff
MEOP = maximum expected operating pressure
MPL = minimum power level
OFT = Orbiter flight test
psf = lb/ft^2
psi = lb/in.^{2}
SRB = solid rocket booster
SRM = solid rocket motor
SSME = Space Shuttle main engine
SSV = Space Shuttle vehicle
STS = Space Transportation System
TPS = thermal protection system
WTR = Western rest range

Presented as Paper 86-0193 at the AIAA 24th Aerospace Sciences Meeting, Reno, NV, Jan. 6–9, 1986; received April 21, 1986; revision received Feb. 9, 1987.

*Aerospace Engineer. Member AIAA.

Introduction

THE complexity of the four-body Space Shuttle vehicle has challenged trajectory designers to define atmospheric ascent flight profiles that will maximize vehicle performance while satisfying vehicle systems constraints. Performance trades of the early 1970's had addressed the performance advantages associated with the Space Shuttle vehicle attitude during the first-stage atmospheric flight and showed that for the anticipated Space Shuttle vehicle trajectory design criteria, a heads-down ascent resulted in 3000 lb more lift capability when compared to a heads-up ascent.[1] An examination of the 1985 Shuttle operational design parameter shows a significant departure from the design parameters of the early Space Shuttle vehicle design phase. Of significance are the results of the SRB certification program that allowed for a 66 psi increase in SRB MEOP.[2] In addition, a negative 5 deg bias to the nominal trajectory design angle of attack during maximum dynamic pressure has occurred. The more negative angle-of-attack design requirement has been precipitated by several factors. The most recent factors are the results of the OFT program, which showed the Orbiter wing loading to be significantly higher than predicted.[3] Although the STS lift capability has increased since STS-1, the changes in design angle of attack have hindered STS lift capability objectives for specific mission out of the WTR launch site. As a result, the ascent performance community is being challenged to increase the STS lift capability at the WTR. This challenge is complicated by the need to minimize all impacts on the operational capability of the STS. This paper addresses a performance enhancement proposal that meets this challenge. The proposal prescribes that the Shuttle ascent trajectory fly a heads-up attitude through the atmospheric portion of first-stage ascent. This proposal will take advantage of the aerodynamic normal force acting on the Space Shuttle vehicle during flight through the atmosphere and permit a 7% increase in the SRM burnrate and a corresponding 4000 lb increase in STS lift capability.

Method of Analysis

Scope of Analysis

A thorough analysis of the performance trades associated with the design angle of attack of the early design phase and the current shuttle operational era is used to explain the trajectory design relationships that now make a heads-up ascent through the atmospheric portion of flight more desirable. This paper investigates the heads-up and heads-down performance trades to angle of attack and dynamic pressure to determine if the heads-up ascent will maintain a desirable performance gain as these trajectory design parameters are changed. This paper also addresses the heads-up and heads-down performance trades associated with the FWC SRB, 109% SSME power level, 50% SSME power level, and the stretched ET to determine if these system-elements performance enhancements are compatible with the proposed heads-up ascent.

Systems Modeling

Heads-up and heads-down ascent trajectory simulations were obtained using a 3 degree-of-freedom, static-moment balance, general trajectory-shaping program. To accurately determine the shuttle operational performance capability, it was necessary to define and model the appropriate shuttle operational subsystem elements. These included first- and second-stage aerodynamics, SSME and SRB propulsion characteristics, SSV control elements, mated vehicle mass properties, and WTR environmental characteristics (winds, atmosphere, gravity).[4-6]

Trajectory Design Requirements

First-stage nominal trajectory design requirements specify that the nominal trajectory be protected for 95 percentile winds dispersions and 90 percentile subsystem dispersions. This is accomplished by designing a mission-unique angle of attack, angle of sideslip, and dynamic pressure vs Mach history. Figure 1 shows typical nominal design profiles for each of these trajectory design parameters. As illustrated, the angle-of-attack profile required to maintain vehicle load margins is in the shape of a bucket with the minimum angle of attack of −5 deg occurring during the maximum dynamic-pressure portion of the trajectory. The angle of sideslip is maintained at 0 deg because of Space Shuttle vehicle symmetry about the yaw plane. The dynamic-pressure constraint required to protect the TPS tiles is achieved by throttling the SSME's. An iterative numerical procedure is used to find the throttle-down and throttle-up times that will satisfy the dynamic-pressure constraint while providing maximum lift capability. The SSME throttle profile must also satisfy the SSME throttle vs altitude constraints as shown in Fig. 2. In addition to these shaping requirements, it is necessary that the staging conditions provide safe SRB separation and SRB recovery. Table 1 shows that SRB separation is sensitive to dynamic pressure, angle of attack, and angle of sideslip, and that SRB recovery is sensitive to SRB-staging apogee altitude (apogee altitude is defined by staging vector).

Trajectory Optimization

After the Space Shuttle vehicle clears the launch tower, a roll maneuver is performed to obtain the desired flight azimuth. During this short period of flight, the Space Shuttle vehicle body attitude is determined by the initial body attitude at tower clearance and the desired body attitude at the end of the roll. Equations (1–5) depict the matrix transformations for the wind, body, and inertial axis systems. These representative equations show that the body attitude of the SSV after the roll maneuver can be determined by knowledge of the instantaneous flight path and the desired values of angle of attack, angle of sideslip, and bank (matrix defined by pitch, yaw, and roll Euler sequence).

$$[I] = [\mathrm{WIT}]_{(\gamma, A_Z, 0)} \times [W] \tag{1}$$

$$[W] = [\mathrm{BWT}]_{(x, \beta, \mu)} \times [B] \tag{2}$$

$$[I] = [\mathrm{WIT}] \times [\mathrm{BWT}] \times [\mathrm{B}] \tag{3}$$

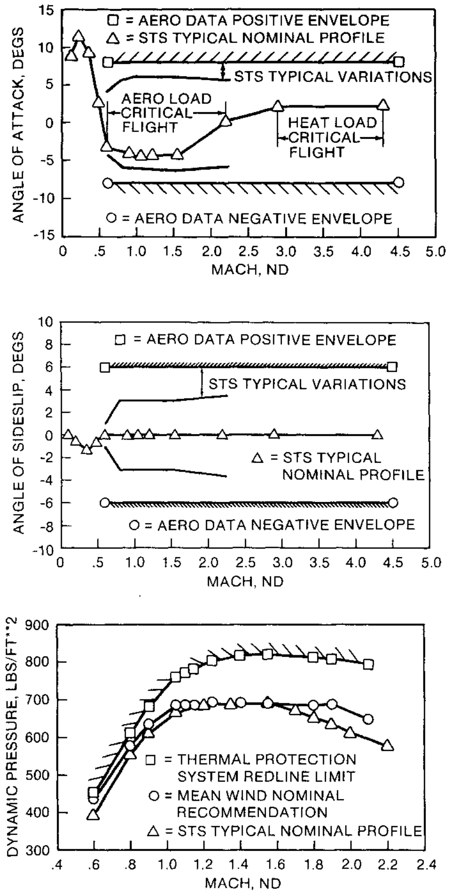

Fig. 1 Typical design profile for STS trajectory parameters.

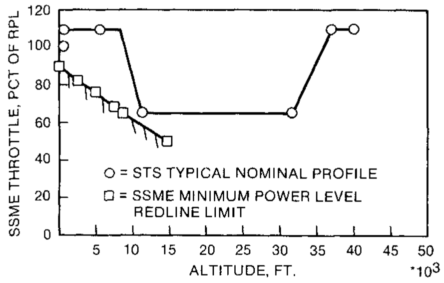

Fig. 2 SSME throttle vs altitude redline.

Table 1 STS SRB staging requirements

Item	Nominal allowance	Typical nominal	Comment
SRB apogee, ft	275000	235000	Chute deploy for SRB recovery
Staging dynamic pressure, lbs/ft^2	45	25	SRB separation
Staging angle of attack, deg	±10	2	SRB separation
Staging angle of sideslip, deg	±10	0	SRB separation

$$[I] = [\mathrm{BIT}]_{(\theta, \psi, \phi)} \times [B] \tag{4}$$

$$[\mathrm{BIT}]_{(\theta, \psi, \phi)} = [\mathrm{WIT}]_{(\gamma, A_Z, 0)} \times [\mathrm{BWT}]_{(\alpha, \beta, \mu)} \tag{5}$$

Since the inertial body attitude of the Space Shuttle is determined by the desired aerodynamic attitudes, staging conditions are primarily influenced by the initial body attitude after the roll maneuver. This type of first-stage trajectory is commonly referred to as an open-loop gravity turn trajectory, since the Earth gravity force is responsible for turning the trajectory and the attitude after the roll maneuver is an open variable. The second-stage trajectory is initialized after SRB separation and uses a closed-loop guidance algorithm to fly the trajectory from the staging state-vector conditions to the desired MECO state-vector conditions. The second-stage powered explicit guidance routines continuously update the Space Shuttle vehicle body attitude to fly a trajectory that will minimize the velocity losses encountered during this portion of flight. It is important to realize that the body attitude after the end of the roll will determine the first-stage trajectory conditions and that these staging conditions will have a direct influence on the second-stage velocity losses. To minimize both the first- and second-stage velocity losses, the desired body attitude at the completion of the roll maneuver is varied in a numerically iterative procedure until a trajectory with minimized summed velocity losses is obtained. Figure 3 depicts typical attitudes for an optimized heads-up and heads-down ascent after the completion of the roll maneuver.

Results

Heads-Down vs Heads-Up Performance

Figure 4 depicts the historical evolution of the Space Shuttle vehicle design angle of attack during maximum dynamic pressure. As shown, the current trajectory design angle of attack is 5 deg more negative than the 1970's design phase angle of attack. Figure 5 depicts the heads-down vs heads-up performance trades, in terms of MECO weight, associated with these changes in design angle of attack. Unlike the design phase studies, the present study varied SRM burnrate as required to take full advantage of the SSME throttle capability and provide maximum lift capability. The data presented in Fig. 5 highlight the heads-up and heads-down performance data at a 0.360 ips SRM burnrate (a 950 psi design phase SRM MEOP). At this burnrate, the current study results generally agree with the design phase results and show that for an angle of attack of +2 and −5 deg, respectively, the heads-down trajectory will provide 1000–3000 lb more lift capability than a heads-up trajectory. However, if the SRM burnrate is increased above 0.368 ips and the design angle of attack is biased to more negative values, the heads-up trajectory will provide more lift capability than a heads-down trajectory. Specifically for the current operational nominal design angle of attack of −5 deg and dynamic pressure of 690 psf (lb/ft^2), a heads-up ascent can accommodate a 0.024 ips increase in SRM burnrate when compared to a heads-down ascent. At this increased burnrate, the heads-up ascent will increase STS lift capability by 4000 lb.

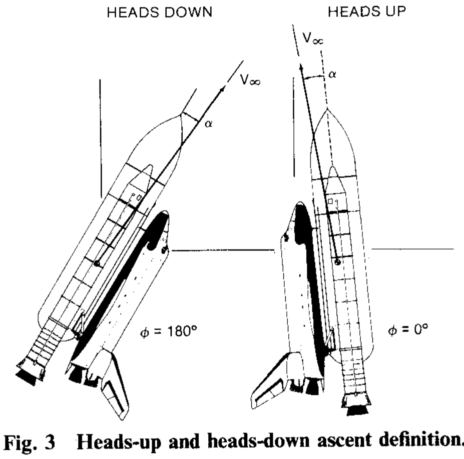

Fig. 3 Heads-up and heads-down ascent definition.

Effects of Angle of Attack for Heads-Down Flight

In the previous section, it was observed that for a heads-down trajectory the lift capability decreased as the nominal angle of attack during maximum dynamic pressure was made more negative. Figure 6 illustrates the atmospheric effects that cause this to happen. Figure 6 also shows that a change in angle of attack from +2 to −5 deg will result in a change in direction of the aerodynamic normal force and causes the resultant external force vector to fall further away from the relative velocity vector. This lag of the external force vector causes the gravity turn trajectory to tilt over at a slower rate. Figure 7 shows how the reduced gravity turn rate affects the flight path and altitude history of the optimized heads-down trajectory. As illustrated, a trajectory design to a more negative angle of attack produces an optimized trajectory with a more depressed flight path at the end of the roll maneuver. This depressed flight path is maintained for the first 60 s of flight through maximum dynamic pressure. As a result, the optimized trajectory flies a lower-altitude profile and encounters a denser atmosphere profile. This requires reduced SRM burnrate (at full SSME throttle capability) to achieve the desired dynamic-pressure constraint and maximized lift capability (defines the performance optimum SRM burnrate). The reduced SRM impulse increases the trajectory gravity losses. The net effect is a reduction in STS lift capability as the design angle of attack is biased more negatively for a heads-down ascent.

Effects of Angle of Attack for Heads-Up

With the insight to understand the effects of angle of attack for a heads-down ascent, it becomes apparent that the heads-up ascent will experience the opposite effects to changes in angle of attack. Indeed the flight-path-angle time-history data presented in Fig. 7 show that for a heads-up ascent the optimized trajectory will fly a more lofted flight profile (prior to maximum dynamic pressure) since the nominal design angle of

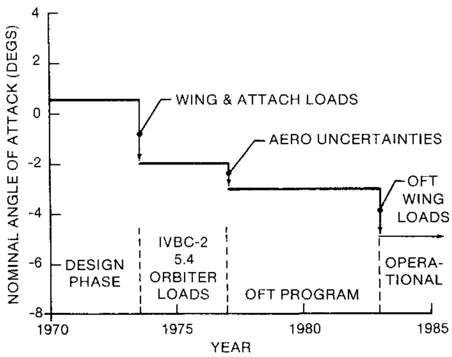

Fig. 4 STS historical nominal design angle of attack.

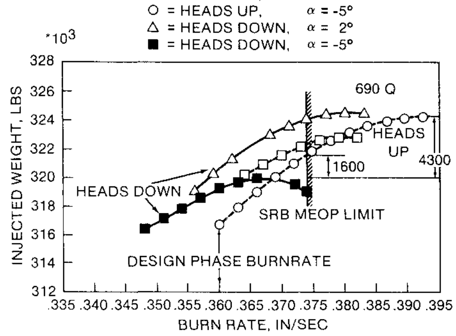

Fig. 5 STS heads-up/down performance vs design angle of attack; in retrospect.

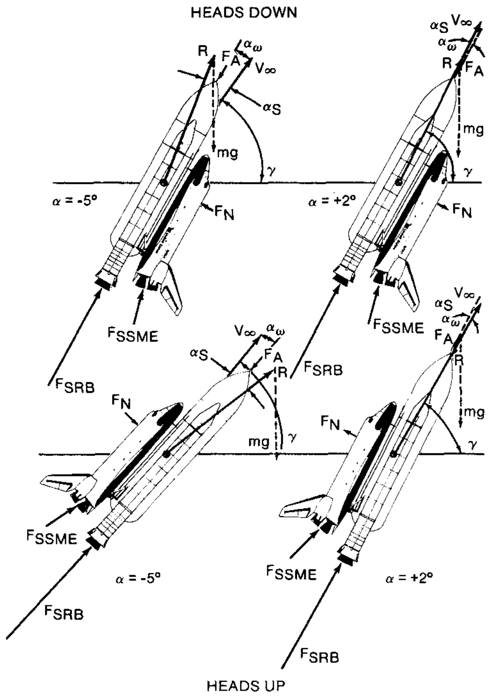

Fig. 6 STS atmospheric flight effects vs angle of attack.

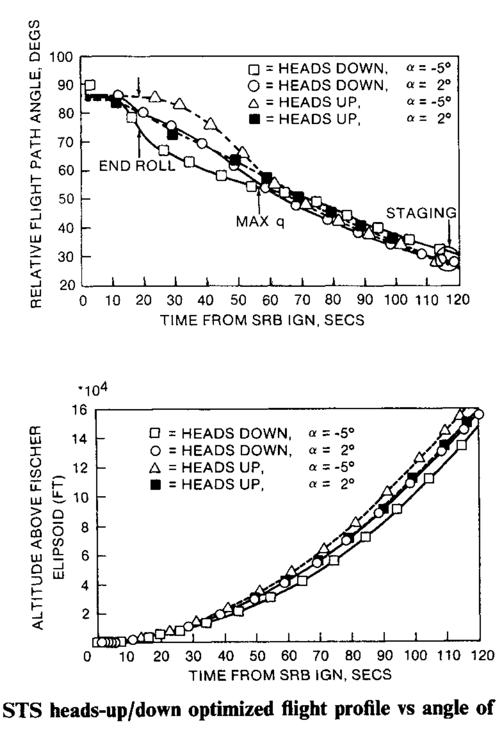

Fig. 7 STS heads-up/down optimized flight profile vs angle of attack.

attack during maximum dynamic pressure is biased to more negative values. This results in the desired tolerance for increases in STS SRM burnrate and the corresponding increase in STS lift capability. The heads-up trajectory at a -5 deg angle of attack and 690 psf dynamic pressure is able to satisfy the trajectory design constraints and permit an increase in SRM burnrate of 0.024 ips and an increase in STS lift capability of 4000 lb. To obtain the same performance gain, a heads-down trajectory would require structural capability that would permit the Space Shuttle vehicle to fly at a $+2$ deg angle of attack in addition to a SRM burnrate definition of 0.383 ips.

Performance Effects of Increased SRM Burning Rate

Figure 8 shows the thrust and flowrate characteristics vs time from SRB ignition at a burnrate of 0.368 ips. The results presented in the previous section scaled this HPM thrust and flowrate data assuming a constant SRM specific impulse and SRB weight vs SRM burnrate. Performance predictions for the SRM at the proposed 0.392 ips are addressed in this section. The data presented in Fig. 9 show that increases in solid SRM burnrate are obtained by increasing the propellant iron oxide content. To obtain the 0.392 ips SRM burnrate, the current SRM propellant iron oxide content would have to be increased from 0.3–0.6%. An SRM burnrate of 0.392 ips results in a SRM MEOP that is 84 psi above the current SRM design capability of 1016 psi, and as a result, structural modifications to the SRM case and SRM nozzle will be required to maintain SRB margins of safety. Figure 10 shows the predicted SRB weight growth required to accommodate SRB margins of safety at increased SRM burnrate. At a SRM burnrate of 0.392 ips, a 2800 lb weight increase per SRB is predicted. In addition, SRM performance characteristics are expected to change as SRM burnrate is increased. The data presented in Fig. 11 show the effects of increased iron oxide content on SRM propellant weight, specific impulse, and total impulse. As shown, only a 0.5 s decrease in specific impulse is predicted for a 0.392 ips SRM burnrate. The predicted SRM performance

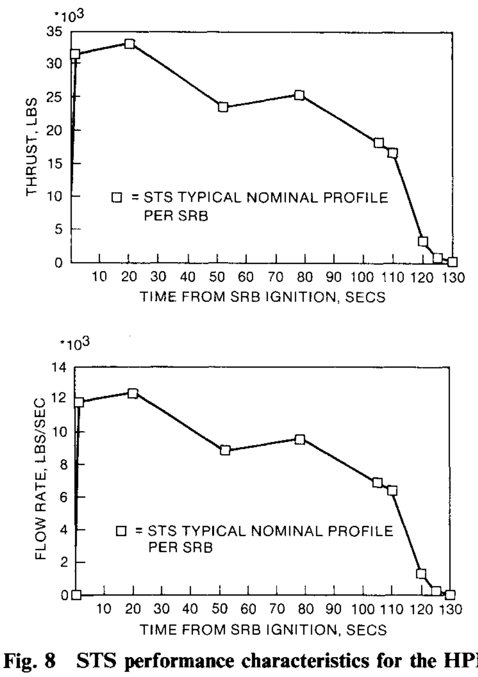

Fig. 8 STS performance characteristics for the HPM.

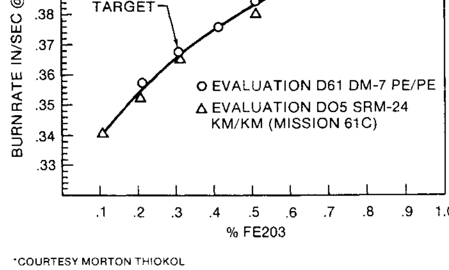

Fig. 9 STS SRM burning rate vs propellant iron oxide content.

characteristics and SRB weight growth were found to reduce the heads-up ascent performance by 850 lb at a 0.392 ips SRM burnrate. The majority (700 lb) of the performance loss is attributable to the increase in SRB case weight.

Attitude Optimization

The performance trades studies of the previous sections assumed a heads-up attitude after the first-stage tilt maneuver and through SRB staging. Additional performance trades studies varying the time to start and end the heads-up attitude were conducted to determine if an additional performance gain existed. The results presented in Fig. 12 show that an additional 950 lb performance gain is realized by having the heads-up trajectory roll to heads-down after maximum dynamic pressure or 60–75 s into the flight. Table 2 shows that the roll to heads-down decreased the second-stage velocity steering losses while producing equal but opposite magnitude changes in velocity drag and gravity losses. It was observed that the roll to heads-down produces a trajectory thrust vector attitude postmaximum dynamic pressure that is more akin to the second-stage closed-loop optimized thrust vector attitude and that this effect provided the decreased steering losses.

STS Trajectory Design Performance Trades

Dynamic Pressure Trades

Heads-down performance trades show a significant change in STS lift capability for changes in design dynamic pressure. Examination of the data presented in Fig. 13 shows approximately a 1800 lb increase in STS lift capability for a 30 psf increase in nominal dynamic pressure. For a heads-down ascent, it was observed that throttling the SSME's to control dynamic pressure had the effect of lofting the optimum trajectory during maximum dynamic pressure. This worked in conjunction with the SSME throttle to constrain dynamic pressure. For a heads-up ascent, the opposite was observed to be true. An investigation of the heads-up performance trades for dynamic pressure shows that this effect was noticeable but small. The heads-up and heads-down performance trades for dynamic pressure at optimized SRM burnrates are summarized in Table 3. Table 3 shows that the heads-up ascent yields 75% of the heads-down performance for a 30 psf change in design dynamic pressure. This will decrease the heads-up vs heads-

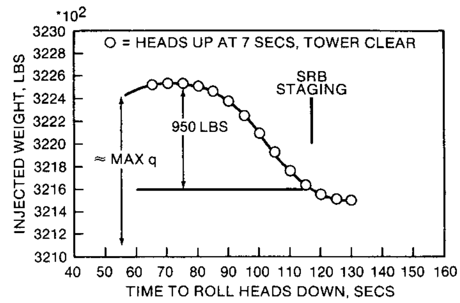

Fig. 12 STS heads-up performance vs time to roll heads-down.

Table 2 Heads-up velocity losses comparisons

	Item	Heads-up down at STG	Heads-up down at 75 s
First- and second stage velocity losses	Gravity, ft/s	4045	4035
	Steering, ft/s	822	766
	Aero, ft/s	326	336

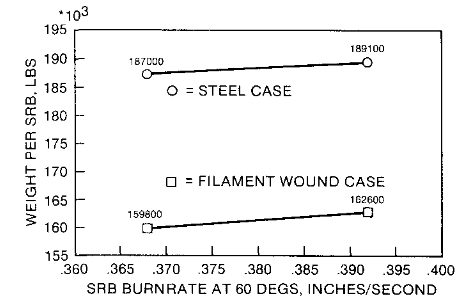

Fig. 10 STS-predicted SRB case weight vs SRM burnrate.

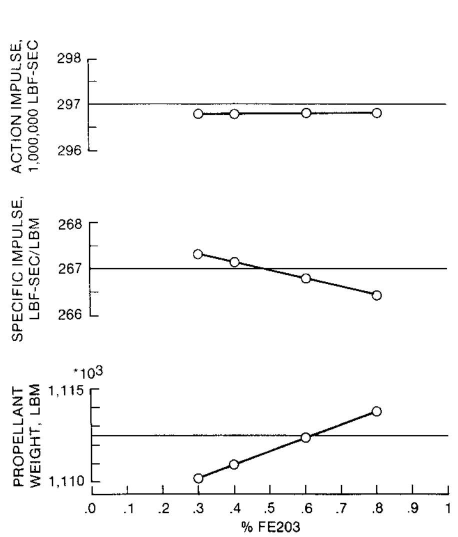

*COURTESY MORTON THIOKOL

Fig. 11 STS-predicted SRM characteristics vs propellant iron oxide content.

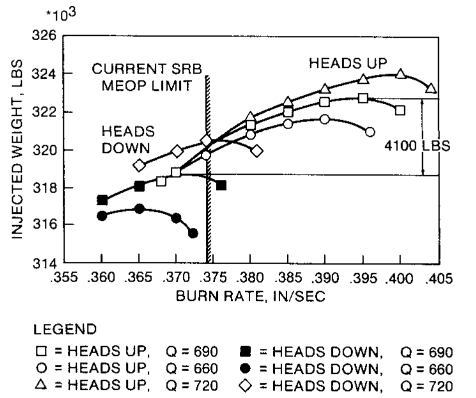

Fig. 13 STS heads-up/down performance trades for dynamic pressure.

Table 3 Heads-up and heads-down dynamic-pressure performance trades

Item	Heads up[a] Δ performance, lbs	Heads down[a] Δ performance, lbs
+30 psf dynamic pressure	1200	1800
−30 psf dynamic pressure	−1300	−1800

[a]Deltas at optimized SRB burnrate.

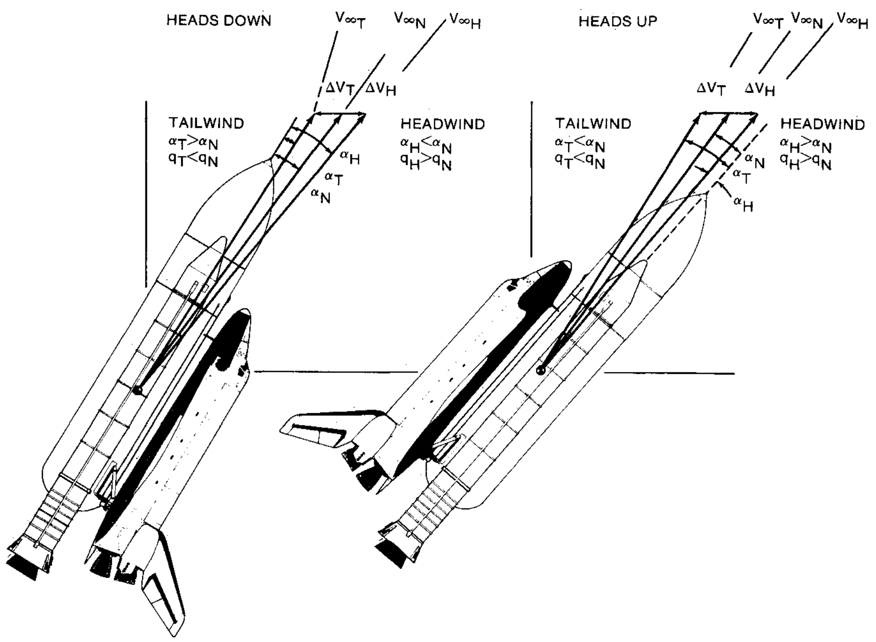

Fig. 14 STS heads-up/down angle-of-attack response to inplane wind dispersions.

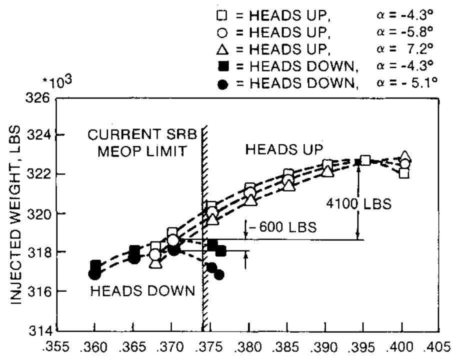

Fig. 15 STS heads-up/down performance trades for angle of attack.

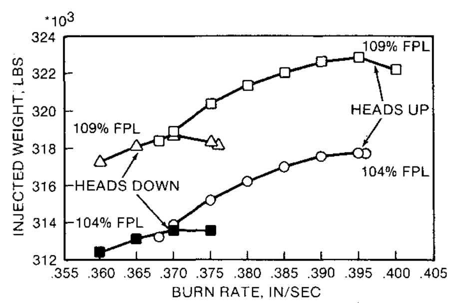

Fig. 17 STS heads-up/down performance trades for maximum SSME power level.

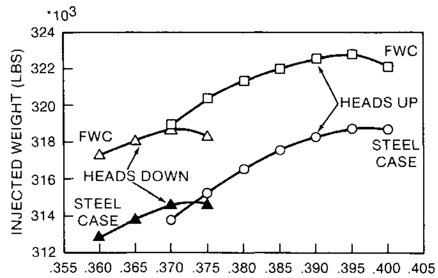

Fig. 16 STS heads-up/down performance trades for the FWC and steel-case SRB.

down performance advantage by 600 lb at 720 psf dynamic pressure and increase the heads-up vs heads-down performance advantage by 600 lb at 660 psf dynamic pressure.

Angle-of-Attack Trades

As schematically shown in Fig. 14, the heads-up trajectory will reverse the Space Shuttle's angle-of-attack sensitivity to inplane wind variations. To accommodate this reversal in wind response and provide the same dispersed load margins as a heads-down trajectory, the heads-up trajectory will be required to fly more negative values of angle of attack. As a result, an analysis of the heads-up performance sensitivity to design angle of attack was pursued. The results presented in Fig. 15 show that at optimized SRM burnrates a heads-up ascent shows a 100 lb change in STS lift capability vs angle of attack when compared to a heads-down ascent. These performance trades show that if a 0.392 ips SRM burnrate is selected, the heads-up performance capability will remain near constant for changes in design angle of attack of 3 deg or less.

STS Systems-Element Performance Trades

Element Trades

The reduced weight of the FWC SRB and the increased thrust of 109% SSME power level represent critical performance enhancements for the STS. In addition, there are other STS performance enhancements that might be implemented. This paper investigated two candidates, an SSME capability of 50% of MPL and a 50 in. stretched ET, in addition to the FWC and 109% SSME, to determine if they are compatible with the proposed heads-up ascent. Figures 16 and 17 show the heads-up and heads-down performance trades vs SRM burnrate for FWC SRB's and 109% SSME. Table 4 summarizes the heads-up and heads-down ascent performance results at optimized SRM burnrates. As shown, for a heads-up ascent only a 50% yield was realized for 50% MPL, whereas a 75% yield was observed for the stretched ET. However, close to 100% yield was observed for the FWC SRB and 109% SSME. These last two elements produce a significant 4000 and 5000 lb increase in lift capability, respectively.

Table 4 Heads-up and heads-down performance trades for element performance enhancements

Item	Heads down[a] Δ performance, lbs	Heads up[a] Δ performance, lbs
50% SSME	1400	700
50 in. stretched external tank	1900	1500
FWC vs steel case	4000	4100
109% SSME vs 104% SSME	4950	5050

[a]Deltas at optimized SRB burnrate.

Conclusions

The results of this paper show that for current Space Shuttle design angle of attack of −5 deg (during maximum dynamic pressure) and design dynamic pressure of 690 psf, a heads-up ascent can accommodate SRB burnrate increases to 0.392 ips and, as a result, can increase the present STS lift capability by 4000 lb. This proposed SRM burnrate is well within the demonstrated SRM technology, but would require SRB modification to maintain SRB margins of safety. In addition, it was shown that a heads-up design maintains positive performance trades for key trajectory design parameters as well as key system-element performance parameters. Data presented show a heads-up ascent will increase the STS lift capability by 3600 lb at 720 psf dynamic pressure and 4600 lb at 660 psf dynamic pressure when compared to a heads-down ascent. It was observed that the heads-up trajectory is performance-insensitive to angle-of-attack changes at the proposed SRM burnrate. The angle-of-attack performance trades are good news if we consider that the heads-up ascent trajectory will require a nominal design to more negative angle of attack to provide the same operational load margins as the heads-down ascent trajectory. Nominal staging conditions for the heads-up ascent will be well within the defined requirements for SRB staging and SRB recovery. The heads-up ascent has the potential to reduce STS FWC and 109% SSME requirements and the ability to increase STS monetary revenues at the ETR launch site. This analysis shows that atmospheric flight of nonsymmetric multibody stages is performance-sensitive to vehicle attitude, trajectory design criteria, and first-stage impulse. Future ground-launched vehicles need to continue to address these design parameters to ensure that maximum performance capability will be achieved.

Acknowledgments

We would like to thank the following individuals for their assistance: Georgia Jarrell, NASA Johnson Space Center; OMNIPLAN Corporation, Houston, Texas; John P. Masetta, NASA Johnson Space Center; for heads-up trajectories, and Charlie Sadderholm, Morton Thiokol, Utah, for SRB performance data at 392 ips, and Lambert Austin, NASA JSC, for paper review.

References

[1]Redd, B., "Orbiter Up/Down Launch Performance Comparison," NASA Memo. EX23/7205–111B, May 1972.

[2]Speak, C. A., Wilks, R. K., and Jones, K. W., "Space Shuttle SRM Performance Improvement," CPI Publication 340, JANAFF Conf., May 1981, pp. 527–542.

[3]Wallace, R. O. et al., "The Space Shuttle Launch Vehicle Aerodynamic Verification Challenges," Space Shuttle Tech. Conf. Rept. 2342, Pt. 1, June 1983, pp. 177–188.

[4]Surber, T. E. and Bornemann, W. E., *Aerodynamic Design Data Book*, Vol. 2, Launch Vehicle IVBC-3, Aug. 1983.

[5]Turner, R. E. and Hill, C. K., "Terrestrial Environment Criteria Guidelines for Use in Aerospace Vehicle Development," NASA TM 82473, 1982.

[6]Mistrot, J. W., "Shuttle Operational Data Book," Vol. 1, Shuttle Systems Performance and Constraints Data, Sept. 1982.

Notice to Subscribers

We apologize that this issue was mailed to you late. As you may know, AIAA recently relocated its headquarters staff from New York, N.Y. to Washington, D.C., and this has caused some unavoidable disruption of staff operations. We will be able to make up some of the lost time each month and should be back to our normal schedule, with larger issues, in just a few months. In the meanwhile, we appreciate your patience.